Proceedings of the 10th World Congress on Civil, Structural, and Environmental Engineering (CSEE 2025)
Barcelona, Spain - April, 2025
Paper No. ICGRE 193
DOI: 10.11159/icgre25.193

Numerical Evaluation of Ground Deformation Due To Thermally Stressed Coal Measure Rock in Underground Coal Gasification

Sandeep Panchal[1], Nikhil N. Sirdesai[2], Abhishek K. Mehadia[3], Sumant Mohanto[4]
[1]Department of Mining Engineering, VNIT Nagpur, India, sandeeppanchal@mng.vnit.ac.in
[2]Department of Mining Engineering, VNIT Nagpur, India, nikhilsirdesai@mng.vnit.ac.in
[3]Department of Mining Engineering, VNIT Nagpur, India, abhimehadia@gmail.com
[4]Department of Mining Engineering, VNIT Nagpur, India, sumantmohanto@mng.vnit.ac.in

Abstract **-** The global energy demand is rising while fossil fuel reserves are decreasing, prompting innovation in resource recovery technologies in the energy sector across the world. Underground coal gasification (UCG) is one such innovation, converting coal into synthetic gas within the earth's crust. However, UCG leaves large cavities, exposing surrounding strata to high temperatures, causing physical and geo-mechanical changes in rock and eventual subsidence. In this paper, a parametric study of UCG reactor cavities of different widths at depths of 100 m, 500 m, and 1000 m with coal seam thicknesses of 1 m, 4 m, 10 m, and 20 m is numerically simulated. Results show that, vertical displacement is directly proportional to the width of the UCG cavity and the thickness of the seam. Highest vertical displacement is found to be 1684.43 mm in case of 50 m wide cavity with 20 m thick coal seam at 1000 m depth. The vertical displacement increased by 5.21% to 7.93%, and horizontal displacement by an average of 6.17%.

Keywords**:** Underground Coal Gasification, Temperature, FEM, Vertical displacement, Horizontal displacement

1. Introduction

The constant increase in the energy demands over the world and limited availability of fossil fuels has become vital issue in the energy sector [1]. Coal, formed from buried plants over millions of years, is non-renewable and a major energy source. The target to meet the over growing demand led to the development of technologies to recover the maximum amount of the natural resources. Conventional coal mining methods have limitations, prompting exploration of novel methods like underground coal gasification (UCG), where the deep coal is converted into synthetic gas within the earth crust[2][3]. Minimal waste and versatility make UCG advantageous, bridging resource gaps. UCG involves in-place combustion of coal to produce low-calorific gas, offering access to otherwise un-mineable reserves. Due to the burning of coal, the UCG process leaves large cavities behind and the strata around the cavity is exposed to high temperature for long durations[4]. Furthermore, due to cavity formation, the overlying strata becomes unstable and tend to fail and fill the cavity which leads to subsidence [5]. This prolonged exposure causes significant physical and mechanical changes in the exposed strata which result in thermal stresses [6]. In UCG process, the mechanical properties of rocks, such as elastic modulus, compressive strength, and tensile strength, undergo significant changes with temperature variations, affecting their structural integrity and behaviour. Several researchers have conducted studies to observe the changes in the properties and the mechanism and magnitude of those changes[4] [7-12]. Elastic modulus (E), which measures a material's resistance to elastic deformation, generally decreases above 1000°C due to thermal alteration. Compressive strength, which indicates resistance to compressive loads, shows mixed trends; for specific sandstones, it increases slightly up to 100°C before decreasing, while other sandstones exhibit irregular patterns, with some maintaining strength up to 500°C and others decreasing earlier. Similarly, tensile strength trends vary among sandstone types. Some samples remain unchanged up to 500°C, while others experience a decline. Lü et al. [13] identified phases where strength slightly increases at 300°C due to water and mineral loss, then decreases from thermal expansion and fractures, with a sharp drop at 800–900°C due to macro fissures. Sirdesai et al. (2017) [14] and Sha et al. (2020) [15]found differing trends, with some sandstones showing monotonic decreases, while others increase up to 400°C before dropping sharply beyond 700°C. These variations highlight the complex effects of temperature on rock strength, which is crucial for geological and engineering applications. The studies show that all the above said properties are highly influenced by the nature of thermal treatment. Thus, UCG process causes instability in overlying strata due to cavity formation and thermal alterations evoked by interaction with high temperature, leading to subsidence [7][16]. Over the years, the technical feasibility of UCG has been established through lab experiments and field trials. However, site-specific

operations pose challenges to commercialization due to incomplete knowledge and the high cost of conducting trials. Numerical modelling offers a solution by studying various parameters, performance, and physical aspects of UCG. These models integrate complex factors like geological aspects, spalling, water intrusions, and chemical reactions. Computational models enable understanding of cavity growth, stress distribution, and other operational parameters. Biezen et al. (1994) [17] simplified 3D modelling to predict cavity development, highlighting the impact of spalling. Perkins (2018) [18] developed models to assess operational conditions' effects on cavity growth, noting limited surface impact. However, commercial UCG projects require long-term modelling of the entire process for accurate predictions. Field trials and lab experiments on UCG have yielded minimal data due to the high cost of extraction and challenges in monitoring operating variables. UCG's site-specific nature limits parameter variation. Laboratory scale models study UCG effects on product gas, temperature, and flow rate, optimizing operating conditions. However, lab experiments may not fully represent UCG's complexities. Both lab and field tests lack detailed quantitative data due to extensive instrumentation and trials. UCG operations are highly site-specific, with limited flexibility compared to surface gasifiers due to unique parameters like depth, seam thickness, and quality. Numerical models are sensitive to these parameters and their changes with temperature. Realistic modelling requires consideration of physical properties and their temperature-dependent variations, along with site-specific geology. In spite of the fact that, large numbers of studies have been done on different rocks but specific numerical studies on coal measure rocks are a fewer. There are several proposed sites for underground coal gasification; therefore, it is of paramount importance to study the influence of temperature on the coal measure rocks. The evaluation of strata damage before the UCG process is crucial for success of the project. Therefore, numerical modelling studies can be a medium to evaluate subsidence i.e. vertical displacement and horizontal displacement during the UCG process. In this paper a comprehensive parametric study of UCG reactor cavity is carried out using FEM based numerical modelling tool RS2. The UCG cavity has been numerically simulated for three different depths from the surface i.e. 100 m, 500 m, and 1000 m. For each depth, four different thicknesses of the coal seam namely, 1 m, 4 m, 10 m and 20 m are considered. The UCG cavity has three different widths i.e., 10 m, 20 m and 50 m for each depth and thickness of the coal seam. A total of 72 numerical models have been simulated out of which 36 models are evaluated for the horizontal and vertical displacement of the strata over the excavation before the ignition process has begun. On the other hand, remaining 36 models are studied to evaluate the horizontal and vertical displacement in the strata, after thermal treatment of the host rock effectuated by underlying UCG process. It is observed that, vertical displacement at the surface is directly proportional to the width of the UCG cavity and the thickness of the seam i.e. higher vertical displacement is observed for larger width of the cavities and for increased height of the cavity opening.

2. Material and Numerical Model Formulation

2.1 Material Properties

The material properties of the rocks used in the model are given in the Table 1. The properties of sandstone have been taken from the extensive literature review. Table 1 displays a type of material as 'SS-RT', where 'SS' indicates sandstone and 'RT' indicates 'room temperature' (26^{o}C) at which the properties have been observed in post cooling. Similarly, for 'SS-1000', SS signifies 'sandstone' and the numeric value, '1000' implies 1000^{o}C temperature.

Table 1: Material Properties

Material Type	Unit Weight (kN/m^3)	Young's Modulus (MPa)	Poisson's Ratio	Tensile Strength (MPa)	Friction Angle (degree)	Cohesion (MPa)
SS-RT	22.0	27820	0.28	4.53	50.87	6.77
COAL	12.0	60	0.30	0.018	26.0	0.12
SS-1000	21.3	4530	0.46	1.8	53.75	2.23
SS-800	21.7	11450	0.38	3.2	50.74	3.16
SS-600	22.0	23330	0.28	4.9	57.76	4.57
SS-400	27.0	29320	0.18	5.1	56.71	5.79
SS-200	21.8	25360	0.28	4.6	55.13	5.07

2.2 Loading and Boundary Conditions

In order to apply loads on the model, it is restrained from three sides and freed from the surface i.e. surface pressure is applied on the top and no additional pressure is applied. The bottom horizontal side is supported with roller supports and movement is allowed only in horizontal direction. The two vertical sides are restrained along horizontal direction with roller supports, movement along only y axis is allowed. For ensuring that applied boundary conditions at the surface and sides are not within the influence zone of the excavation operation, the sides are designed fifty times the width of opening and the under burden is thirty percent of the overburden. Also, a gravitational force ($g = 9.81\ m/s^2$) is applied to the model as body force.

2.3 Assumptions

Following assumptions are made for the analysis of the ground behaviour using the finite element modelling:

i. All the finite element models are analysed considering the coal seam to be an undisturbed seam.
ii. The entire system is intact.
iii. In all the models, the coal seams and sandstone layers are completely horizontal.
iv. The material used for modelling is homogenous.
v. The material properties are completely isotropic.
vi. There are no major jointing and faults.
vii. The process in the modelling is completely adiabatic with linear changes in the properties.
viii. The zone variation of temperature is dependent on thermal gradient of the strata.
ix. No ground water influence is considered.
x. No dynamic loading is applied in the model.
xi. The effect of particular joint or bedding plane is not analysed explicitly.
xii. The failure condition is set to 'Mohr Coulomb' for modelling.

2.4 Geometry and Generation of Numerical Model

The numerical simulation process begins with development of the models in 2D in the numerical modelling software, RS2. To cite an example, the models are named as '500T10W10', where '500' signifies the depth of the seam from the surface is 500 m, T10 indicating that the thickness of the coal seam is 10 m and lastly W10 pointing that the width of the cavity is 10 m. Since the dimensions are kept such that, the sides do not lie in the influence zone, the model's width is 100 times the width of the cavity, for a 10 m wide cavity the width is 1010 m (i.e. 10x100 + 10 = 1010) and similarly the under-burden is 0.3 times that of the depth of the seam, hence, for a 500 m deep seam the total model height is 660 m (500 + 10 + 500*0.3 = 660) and likewise in all models. The cavity has been simulated for three different depths from the surface i.e. 100 m, 500 m, and 100 0m. For each depth there are four different thicknesses of the coal seam 1 m, 4 m, 10 m and 20 m represented as T1, T4, T10 and T20 respectively. The UCG cavity has three different widths of 10 m, 20 m and 50 m represented by W10, W20 and W50 for every depth and thickness of the coal seam. A total of 72 models have been designed for the simulation out of which 36 models are evaluated for the horizontal and vertical displacement of the strata over the excavation before the ignition process has been initiated. On the other hand, the remaining 36 models are studied to evaluate the horizontal and vertical displacement in the strata, after the thermal treatment of the host rock due to the process of UCG.

3. Results and Discussions

All the FEM models are analysed based on the non-linear, elastic behaviour of rock material. Results of FEM analyses are obtained in terms of displacement. The displacements are categorized into two categories i.e. vertical displacement and horizontal displacement. The vertical displacement is observed along a vertical line from the centre of the roof of the cavity to the centre of the top surface of the model boundary. The horizontal displacement is observed along the complete surface i.e. along a horizontal line at the surface of the model. The values for the displacement of each FEM model have been recorded separately. The values are determined along a predetermined linear path in the model. The results are classified into

variations of models with thermally altered properties and models without thermal alteration. Variations in displacement with respect to the depth of the seam, width of the opening and thickness of the coal seam have been observed.

3.1 Thermally Unaltered Strata

3.1.1 Vertical Displacement

Fig. 1 illustrates vertical displacement contours of the model for thermally unaltered strata. Maximum displacement takes place at the immediate roof of the cavity and continues to decrease towards the surface. Also, with movement away from the centre line the vertical displacement tends to decrease.

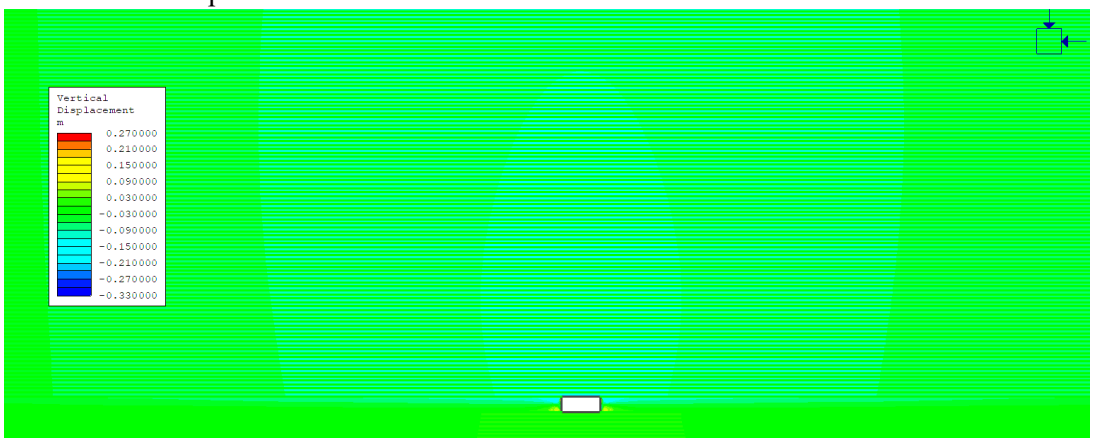

Fig. 1: Vertical displacement contours

3.1.1.1 Based on Width of Opening

With increase in the width of opening there is increase in the vertical displacement on the surface of the model as shown in Fig. 2. At the lower widths (10 m to 20 m) the increase is gradual while, when the width of opening increases to 50 m there is a drastic increase in the surface displacement.

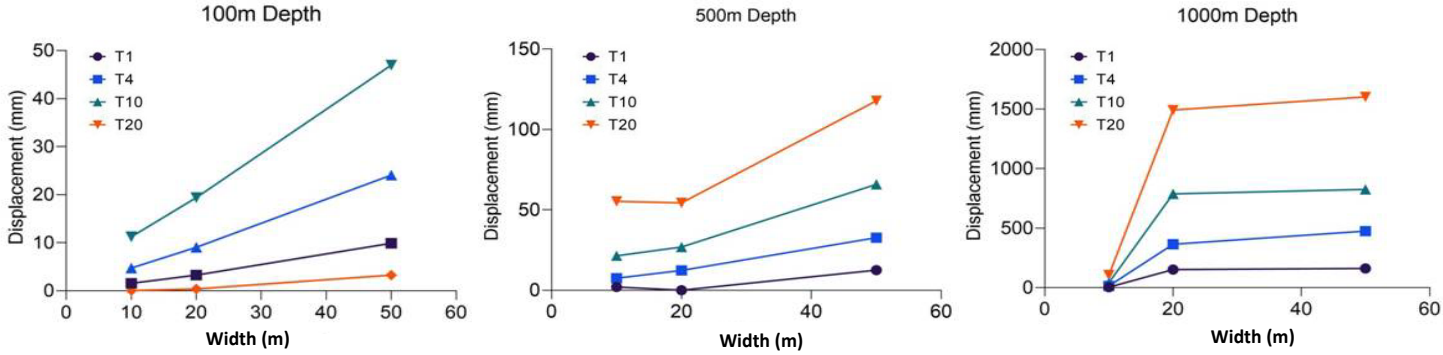

Fig. 2: Plot of vertical displacement (mm) vs width of opening (m) at different depths

The increase in vertical displacement is also clearly visible for a given depth with the increase in the thickness of the coal seam i.e. as the thickness of coal seam increases for the fixed depth there is increase in vertical displacement. On the other hand, there is some anomaly with 20 m thick seams for 100 m depth, where the vertical movement is very less, this behaviour can be justified due to the lateral spalling of the coal seam. From the modelling it was noted that, for a width of 10 m, maximum vertical displacement is observed in 20 m thick seam at 1000 m depth of 105.27 mm, similarly for the 20 m width of opening the maximum vertical displacement is 1498.90 mm at 1000 m depth and 20 m thick seam and for 50 m width the vertical displacement is 1600.93 mm for 1000 m deep and 4 m thick seam.

3.1.1.2 Based on Depth of Seam

It can be evidenced from Fig. 3 that for a certain thickness of coal seam, with increase in the depth of the coal seam, there is increase in the vertical displacement. However, for lower depths (less than 500 m) the vertical displacement is very less than the vertical displacement experienced in depth toward 1000 m. It can also be seen that, for a given thickness and at certain depths of the coal seam, with the increase in the width of the cavity opening there is substantial increase in the vertical displacement magnitude.

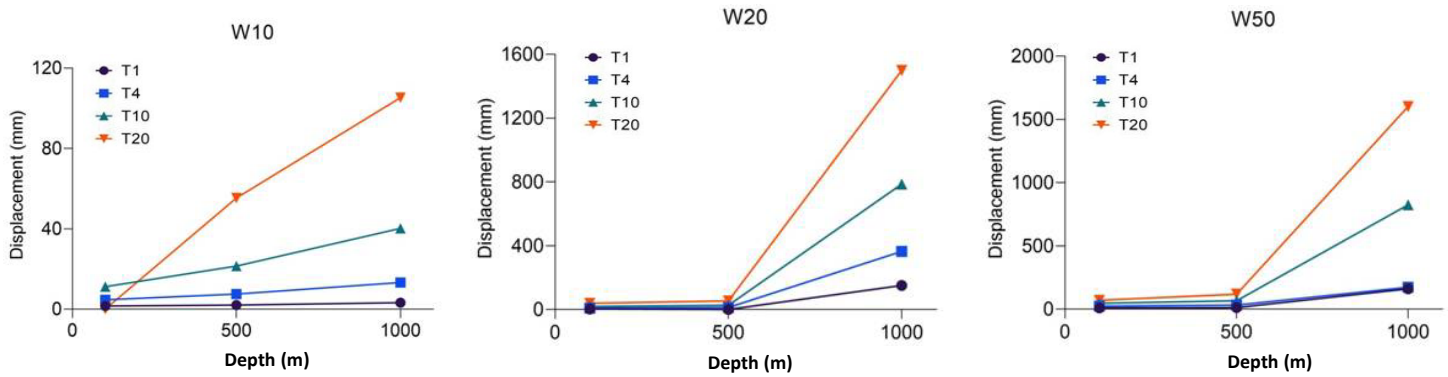

Fig. 3: Plot of vertical displacement (mm) vs depth of seam (m) at different widths

In case of 100 deep seam, maximum vertical displacement is 48.26 mm for 50 m width of opening. A maximum vertical displacement of 117.81 mm is observed for 50 m width and 20 m thickness for 500 m deep excavation. For 1000 m deep excavation vertical displacement of 1600.93 mm is observed for a width and thickness on 50 m and 20 m respectively.

3.1.2. Horizontal Displacement

Fig. 4 depicts horizontal displacement contours of the model for thermally unaltered strata. The maximum displacement can be seen at the side walls of the excavation. The Centre line from the centre of the excavation roof has no horizontal displacement.

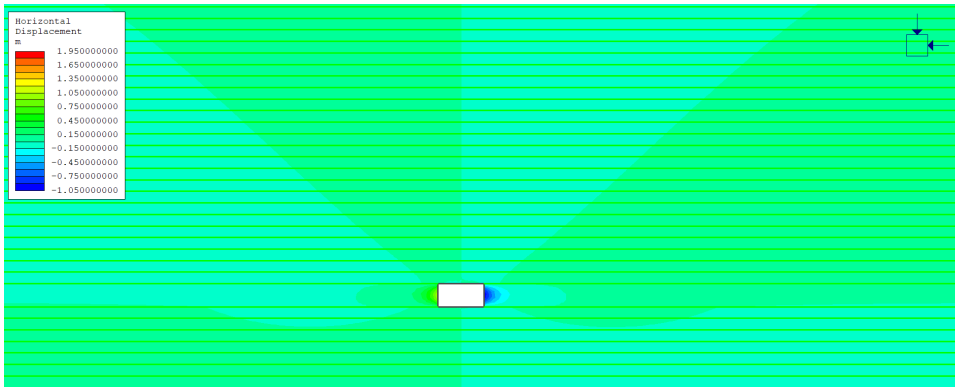

Fig. 4**:** Horizontal displacement contours

It is visible from Fig. 5 that there is zero or negligible horizontal displacement at the corners and at the centre of the model. According to the nomenclature, the left part of the curve shows positive movement of the particle and the right curve shows negative movement horizontally.

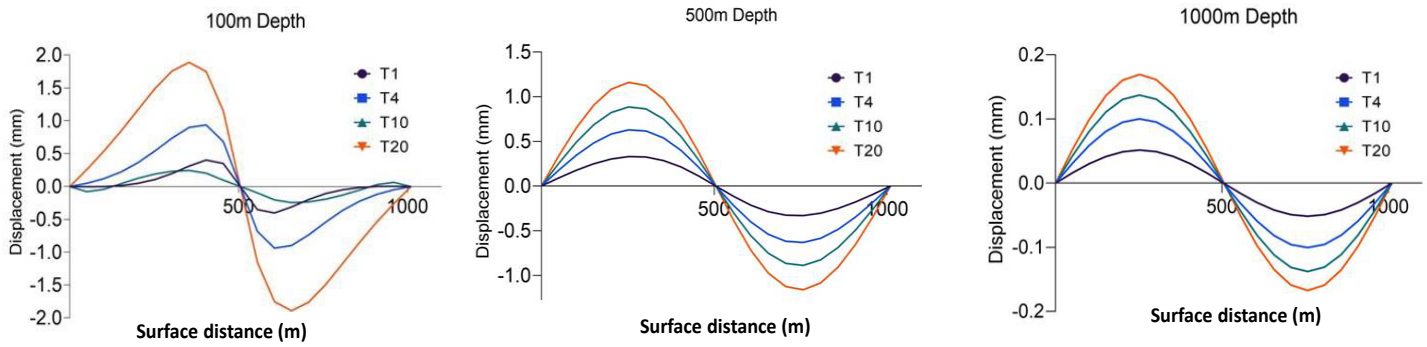

Fig. 5: Plot of horizontal displacement (mm) at surface for 10 m wide opening

For 10 m width of opening, the horizontal displacement decreases with the increase in depth as shown in Fig. 5. Highest horizontal displacement is observed for higher thickness of the seam at lower depths. Similar analysis is carried out for 20 m and 50 m wide cavities. For 100 m depth, 20 m width of opening, the horizontal displacement values are observed low, which can be justified by spalling of coal seam. For 20 m and 50 m width of opening, the horizontal displacement is directly proportional to the depth of seam. Highest horizontal displacement is observed for 1000 m depth. As pet the variations of thickness of coal seam, higher displacements are seen for higher thickness of the seam. When measured, maximum horizontal displacement for a 10 m wide opening is 1.85 mm for a thickness of 10 m and depth of 100 m. For 20 wide opening, maximum displacement of 7.10 mm is observed in 20 m thick and 500 m deep seam. A maximum horizontal displacement of 29.03 mm is observed for 50 wide excavations at 1000 m deep seam and 20 m thickness of seam.

3.2. Thermally Altered Strata

In the thermally modified strata, because of the ignition of the coal, the temperature around the seam has risen and caused irreversible changes in the physical and mechanical properties of the host rock.

3.2.1 Vertical Displacement

The trend in deformation behaviour is found similar to that of the thermally undisturbed strata but the magnitude of displacements is larger due to the decrease in the strength properties of the rock which will be evident in the subsequent sections.

3.2.1.1. Based Width of Opening

The variation of vertical displacement with the width of opening is depicted in Fig. 6. It is clearly visible from the figure that with the increase in the depth of coal seam, there is increase in the vertical displacement. When compared to the unaltered rocks, the graph has similar trends but higher values. With the increase in the width of opening, gradual increase in vertical displacement can be observed.

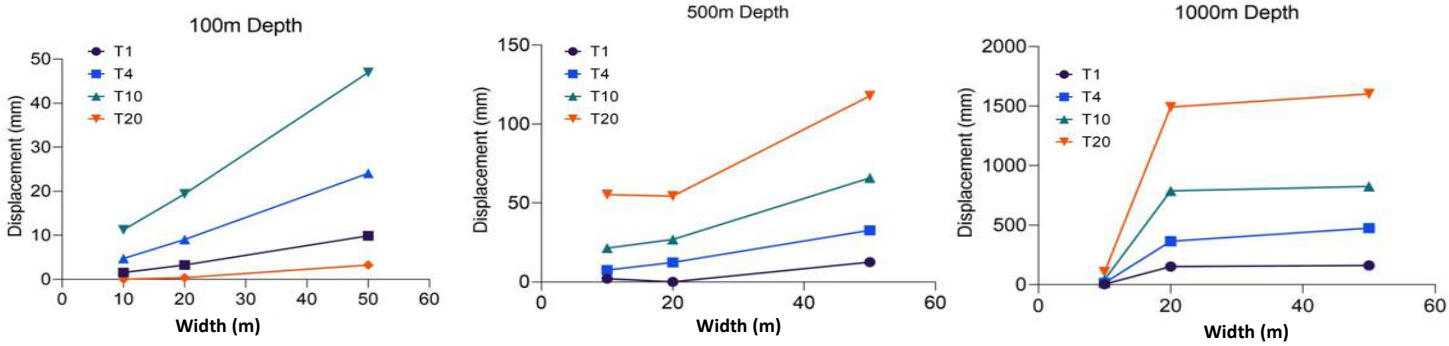

Fig. 6: Plot of vertical displacement (mm) vs width of opening (m) at different depths

For a given depth and width of the opening, as the thickness of coal increases the vertical displacement increases. For the depth of 100 m and 20 m thickness of coal seam, there is a different trend due to the phenomenon of coal bulging. For thermally altered rock, the displacement values are higher than that of thermally unmodified rocks. For the 10 m wide opening, the value rose to 106.79 mm, for 20 m wide opening the increase is to 1514.69 mm and for 50 m wide opening the value increased to 1684.43 mm.

3.2.1.2 Based on Depth of Seam

For a given width of opening, there is an increase in the vertical displacement. However, the magnitude of vertical displacement is lower for shallower seams and increases drastically as the depth increases. It is evident from the Fig. 7 that with the increase in the width of opening for specific thickness of seam, the vertical displacement increases at certain depth.

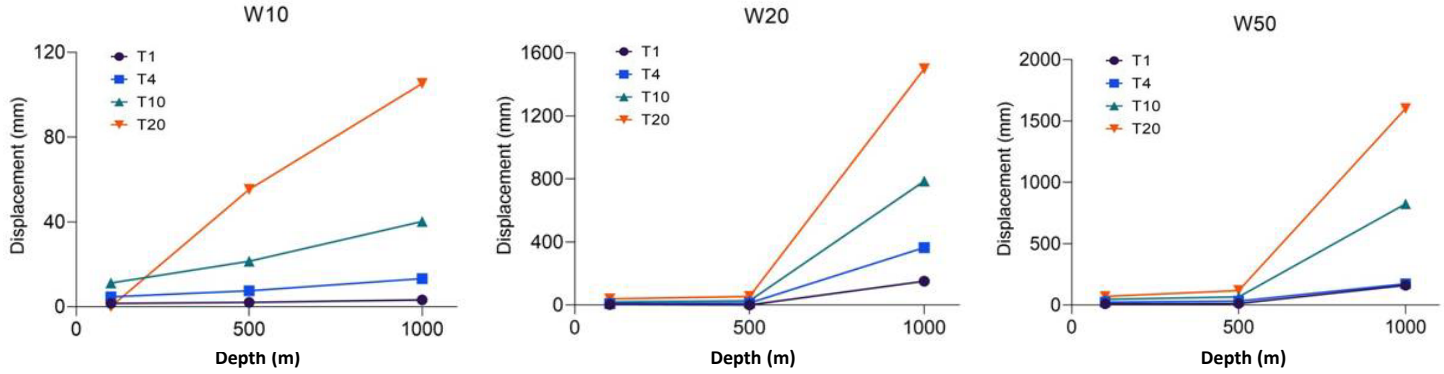

Fig. 7: Plot of vertical displacement (mm) vs depth of seam (m) at different widths

Similar phenomenon of increase in vertical displacement is observed in case of 100 m, 500 m and 1000 m deep seams where vertical displacement magnitude increased to 49.96 mm, 127.16 mm and 1684.43 mm respectively.

3.2.2 Horizontal Displacement

The maximum horizontal movement are observed at the side walls of the excavation similar to unaltered strata. The line from the centre of the excavation roof has no horizontal displacement. Fig. 8 shows the horizontal displacement for the width of 10 m of opening.

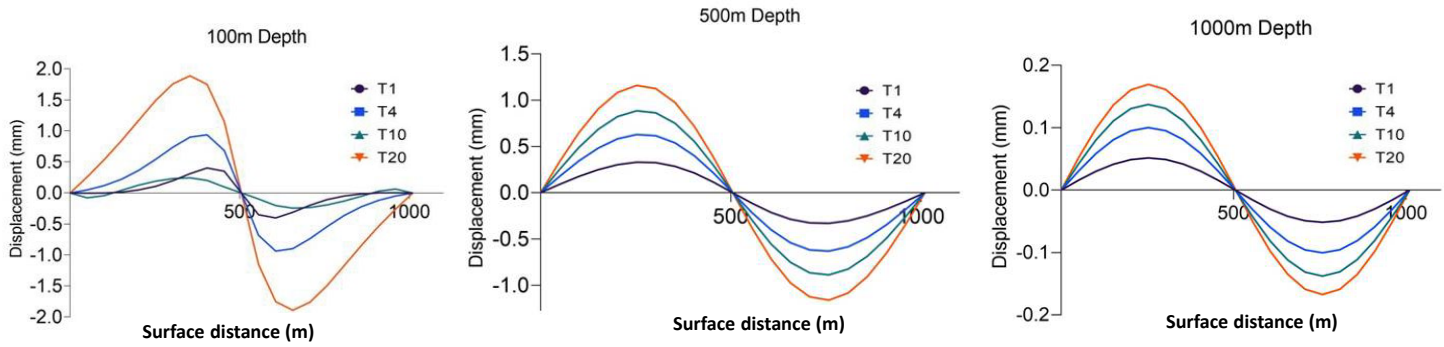

Fig. 8: Plot of horizontal displacement (mm) at surface for 10 m wide opening

Similar to that of the previous section, there is zero or negligible horizontal displacement at the corners and at the centre of the model. As per the nomenclature, the left part of the curve shows positive horizontal movement of the particle and the right curve shows negative horizontal movement. Similar analyses are undertaken for 20 m and 50 m wide openings. For the width of opening of 10 m, the horizontal displacement decreases with the increase in depth of the coal field for a given thickness of seam. While for constant depth, with the increase in thickness of coal seam, there is an increase in displacement. For the horizontal displacement the increments are very marginal. At the depth of 100 m the displacement increases to 1.88

mm. For, 500 m depth, the horizontal displacement is 7.81 mm and finally for 1000 m deep seams it increased to 31.01 mm. For the width of opening of 20 m, the horizontal displacement decreases with the increase in depth of the coal field for a given thickness of seam. While for constant depth, with the increase in thickness of coal seam, there is an increase in the horizontal displacement. For a 50 m opening, maximum horizontal displacement is visible at greater depths. For a certain depth the increment in horizontal displacement is seen with increasing thickness i.e. height of the seam.

4. Conclusion

In order to design the UCG and to reduce the environmental impacts associated with the process, complete information with respect to the strata and its behaviour considering the thermal exposure and excavation dimension appeared to be of paramount significance. The major conclusions drawn from this study are followings:

i. For the same values of physical and mechanical properties of rock, with the increase in width of opening and/or increase in depth of the opening the displacement in the strata increases.
ii. After thermal treatment of coal measure rock, there is increment in displacement values when compared to thermally unaltered strata.
iii. For same widths, maximum increment of about 5.21% is observed between the 2 sets of model and similarly at same depths, an increase in maximum displacement of 7.93% is evidenced.
iv. An average increment of 6.17% is observed in horizontal displacement.

References

[1] X. Yang, C. P. Nielsen, S. Song, and M. B. McElroy, "Breaking the hard-to-abate bottleneck in China's path to carbon neutrality with clean hydrogen," *Nat. Energy*, vol. 7, no. 10, pp. 955–965, 2022.

[2] Z. Yin, H. Xu, Y. Chen, T. Zhao, and J. Wu, "Experimental simulate on hydrogen production of different coals in underground coal gasification," *Int. J. Hydrogen Energy*, vol. 48, no. 19, pp. 6975–6985, 2023.

[3] A. W. Bhutto, A. A. Bazmi, and G. Zahedi, "Underground coal gasification: From fundamentals to applications," *Prog. Energy Combust. Sci.*, vol. 39, no. 1, pp. 189–214, 2013.

[4] L. Jiang, Z. Chen, and S. M. F. Ali, "Thermal-hydro-chemical-mechanical alteration of coal pores in underground coal gasification," *Fuel*, vol. 262, p. 116543, 2020.

[5] H. Kratzsch, *Mining subsidence engineering*. Springer Science & Business Media, 2012.

[6] M. Hajpál and Á. Török, "Mineralogical and colour changes of quartz sandstones by heat," *Environ. Geol.*, vol. 46, pp. 311–322, 2004.

[7] M. Shahbazi, M. Najafi, M. F. Marji, and R. Rafiee, "A thermo-mechanical simulation for the stability analysis of a horizontal wellbore in underground coal gasification," *Petroleum*, vol. 10, no. 2, pp. 243–253, 2024.

[8] H. Tian, T. Kempka, S. Yu, and M. Ziegler, "Mechanical properties of sandstones exposed to high temperature," *Rock Mech. Rock Eng.*, vol. 49, pp. 321–327, 2016.

[9] Q. Tan, X. Luo, and S. Li, "Numerical modeling of thermal stress in a layered rock mass," in *ARMA US Rock Mechanics/Geomechanics Symposium*, ARMA, 2008, p. ARMA-08.

[10] M. Najafi, S. M. E. Jalali, and R. KhaloKakaie, "Thermal–mechanical–numerical analysis of stress distribution in the vicinity of underground coal gasification (UCG) panels," *Int. J. Coal Geol.*, vol. 134, pp. 1–16, 2014.

[11] X. Liu, G. Guo, and H. Li, "Thermo-mechanical coupling numerical simulation method under high temperature heterogeneous rock and application in underground coal gasification," *Energy Explor. Exploit.*, vol. 38, no. 4, pp. 1118–1139, 2020.

[12] H. Tian, T. Kempka, N.-X. Xu, and M. Ziegler, "Physical properties of sandstones after high temperature treatment," *Rock Mech. rock Eng.*, vol. 45, pp. 1113–1117, 2012.

[13] C. Lü, Q. Sun, W. Zhang, J. Geng, Y. Qi, and L. Lu, "The effect of high temperature on tensile strength of sandstone," *Appl. Therm. Eng.*, vol. 111, pp. 573–579, 2017.

[14] N. Sirdesai, "Numerical and experimental study of rocks under very high temperature conditions-Underground coal gasification," Monash University, 2017.

[15] S. Sha, G. Rong, J. Tan, R. He, and B. Li, "Tensile strength and brittleness of sandstone and granite after high-temperature treatment: a review," *Arab. J. Geosci.*, vol. 13, pp. 1–13, 2020.

[16] E. A. Burton, R. Upadhye, and S. J. Friedmann, “Best Practices in Underground Coal Gasification,” Livermore, 2019. doi: https://doi.org/10.2172/1580018.
[17] E. N. J. Biezen, J. Bruining, and J. Molenaar, “An integrated 3D model for underground coal gasification,” in *SPE Annual Technical Conference and Exhibition?*, SPE, 1995, p. SPE-30790.
[18] G. Perkins, “Underground coal gasification–Part II: Fundamental phenomena and modeling,” *Prog. Energy Combust. Sci.*, vol. 67, pp. 234–274, 2018.